International Journal of Biological Macromolecules 106 (2018) 312–319

Contents lists available at ScienceDirect

International Journal of Biological Macromolecules

journal homepage: www.elsevier.com/locate/ijbiomac

Impact of the removal of N-terminal non-structured amino acids on activity and stability of xylanases from *Orpinomyces* sp. PC-2

Rafaela Zandonade Ventorim[a], Tiago Antônio de Oliveira Mendes[b], Larissa Mattos Trevizano[a], Ana Maria dos Santos Camargos[a], Valéria Monteze Guimarães[a,*]

[a] *BIOAGRO, Universidade Federal de Viçosa, Viçosa, MG 36.570000, Brazil*
[b] *Departamento de Bioquímica e Biologia Molecular, Universidade Federal de Viçosa, Viçosa, MG 36.570000, Brazil*

ARTICLE INFO

Article history:
Received 20 April 2017
Received in revised form 19 July 2017
Accepted 1 August 2017
Available online 3 August 2017

Keywords:
Xylanase
Orpinomyces
Thermostability
Molecular dynamics simulation

ABSTRACT

Xylanases catalyze the random hydrolysis of xylan backbone from plant biomass and thus, they have application in the production of biofuels, Kraft pulps biobleaching and feed industry. Here, xylanases derived from *Orpinomyces* sp. PC-2 were engineered guided by molecular dynamics methods to obtain more thermostable enzymes. Based on these models, 27 amino acid residues from the N-terminal were predicted to reduce protein stability and the impact of this removal was validated to two enzyme constructs: small xylanase Wild-Type (SWT) obtained from Wild-Type xylanase (WT) and small xylanase Mutant (SM2) generated from M2 mutant xylanase (V135A, A226T). The tail removal promoted increase in specific activity of purified SWT and SM2, which achieved 5,801.7 and 5,106.8 U mg^{-1} of protein, respectively, while the WT activity was 444.1 U mg^{-1} of protein. WT, SWT and SM2 showed half-life values at 50 °C of 0.8, 2.3 and 29.5 h, respectively. Overall, in view of the results, we propose that the presence of non-structured amino acid in the N-terminal leads to destabilization of the xylanases and may promote less access of the substrate to the active site. Therefore, its removal may promote increased stability and enzymatic activity, interesting properties that make them suitable for biotechnological applications.

1. Introduction

Xylanases (E.C.3.2.1.8) catalyze the random hydrolysis of xylan backbone, a main constituent of plant biomass, in an endwise manner to yield xylooligosaccharides [1]. Due to this remarkable role in the deconstruction of xylan, these enzymes have aroused great interest for the production of biofuels, biobleaching of Kraft pulps and in the feed industry [2].

Xylanases are classified within glycoside hydrolase (GH) families 5, 8, 10, 11, and 30 according to Carbohydrate-Active enZymes (CAZy) database (www.CAZy.org) based on similarities of the catalytic domain sequences [3,4]. Compared to the other families, GH11 xylanases have several interesting properties that make them suitable for biotechnological applications, such as high substrate selectivity, high catalytic efficiency, and activity in a broad ranges of pH and temperature [2].

Xylanases from the same GH family show similar three-dimensional structures, active-site geometries and conserved enzymatic mechanism. The xylanase family 11 present a compact globular structure with a single α-helix and two extended pleated β-sheets forming a jelly-roll fold [5]. The main feature of this family is the presence of a long cleft that spans the entire molecule. This cleft contains the active site including two glutamate residues that directly participate of xylan hydrolysis, in which one acting as acid/base catalyst and the other as a nucleophile [5,6].

GH11 xylanase (XynA) produced by the anaerobic fungus *Orpinomyces* sp. PC-2 showed higher specific activity compared with equivalent enzymes from other sources [7]. This native enzyme was most efficient in the pH ranging from 5.0 to 6.5 and temperatures from 40 to 50 °C [7,8]. However, more stable enzymes are required for biotechnological processes, such as pulp and paper, animal feed and biofuel industries. The xylanases must be suitable for the pH and temperature conditions of these processes, exhibiting high thermostability and wide pH adaptability [2,9].

In our previous work, the directed evolution methodology using the mutagenic technique of error-prone PCR was carried out to improve the thermostability of xylanases derived from *Orpinomyces* XynA [9]. This methodology was effective to identify four mutant xylanases, which exhibited higher thermostability at 60 °C compared to the wild-type enzyme (WT XynA). However, these

* Corresponding author.
E-mail address: vmonteze@ufv.br (V.M. Guimarães).

http://dx.doi.org/10.1016/j.ijbiomac.2017.08.015
0141-8130/

more thermostable mutant enzymes showed drastic reduction of activity. An exception was the M2 mutant xylanase (V135A, A226T) that exhibited a half-life of 33.2 min at 60 °C, approximately four times higher than the wild-type enzyme (7.92 min) and maintained similar activity. Therefore, the M2 mutant xylanase showed to be most promising for future industrial application from the biotechnological point of view.

Several studies have demonstrated the impact of unstructured amino acids, located in the N-terminal region, in the thermostability of xylanases [10,11]. The removal of N-terminal residues by strategies of enzyme rational engineering could promote enhancement of enzyme thermostability. In this work, Molecular Dynamics (MD) approaches were taken to evaluate alterations in the N-terminal region of WT xylanase derived from *Orpinomyces* XynA that could potentially affect protein stability and activity in order to generate improved xylanases and two enzyme constructs were produced to validate the simulation results.

2. Material and methods

2.1. Strains, vectors and reagents

E. coli BL21-CodonPlus (DE3)-RIPL competent cells were purchased from Stratagene (La Jolla, CA, USA) and used for protein expression. The expression vector pET24(b) and the KOD DNA polymerase kit were purchased from Novagen – EMD Millipore (San Diego, CA, USA). The T4 DNA ligase kit and enzymes *Nde*I and *Xho*I were purchased from Fermentas – Thermo Fisher Scientific (Waltham, MA USA). The Gel Extraction DNA kit and DNA plasmidial purification Miniprep kit were purchased from Qiagen (Venlo, Germany). The *E. coli* strain DH5α (Stratagene) was used for propagation and manipulation of plasmids. Beechwood xylan and xylose were purchased from Sigma Chemical Co. (St. Louis, MO, USA).

2.2. Prediction of signal peptides

The SignalP 4.0 server (http://www.cbs.dtu.dk/services/SignalP-4.0/) [12] settled to Eukaryotes was used to predict export peptide signal and cleavage site from *Orpinomyces* XynA xylanase and the ProtParam tool (http://web.expasy.org/protparam/) [13] was used to predict physical and chemical parameters of wilde-type and mutant proteins.

2.3. Xylanase molecular dynamics

The Phyre2 web server (http://www.sbg.bio.ic.ac.uk/phyre2/) [14] was used to obtain the 3D model of the WT XynA catalytic domain and SWT xylanase. As in the previous work [9], the models obtained were constructed based on the xylanase from *Neocallimastix patriciarum* (PDB ID 2C1F, 2.1 Å resolution) [15] that shows 91% identity with the catalytic domain of *Orpinomyces* XynA. Considering this alignment, it was possible to construct a model for residues 13-230 of the wild-type XynA, without signal peptide, and 2-213 of the SWT. The model was checked for their stereochemical and overall structural quality using Phyre2 Investigator [14], Procheck [16], Verify_3D [17,18], ERRAT [19], RAMPAGE [20], ProSA-web [21] and JPred4 [22]. The three-dimensional structure of modeled protein was analyzed using the PyMOL Molecular Graphics System (Version 1.8, Schrödinger, LLC).

Molecular dynamics simulations were carried out on a computer cluster equipped with 2 Intel Xeon processors X5650, 2.66 GHz and 48 GB of RAM on a Linux Platform, using NAMD software (Version 2.11) [23] and performed with CHARMM force field (Version 1.9.2) [24]. VMD interface [25] was used to prepare the xylanase models as well as to make visualizations and analysis of trajectories. The system size was chosen to distance the protein atoms approximately 5.0 Å of the edge of the simulation water box. The systems were minimized at 313 or 323 K for 1000 steps to equilibrate the positional restraints on the proteins with solvent molecules. The final production of simulations were done for 10 ns with the time step of 2 fs at 313 and 323 K. Pressure was controlled with a Langevin piston (1 atm) and temperature by Langevin thermostat. The Particle Mesh Ewald (PME) algorithm [26] was used to model the electrostatic interactions. Trajectories were saved at every 5000 steps.

2.4. Primers construction and PCR amplifications

A pair of oligonucleotides, XF1 (5′GGCAATTCCATATGGGTCAAAGATTAAGCGTTGG3′) and XR1 (5′GCCGCTCGAGTTAACGAGGAGCAGAACCTTGTTT3′), was synthesized to performe amplification of genes encoding the selected xylanases (SWT and SM2). XF1 matched with the nucleotide 85 and XR1 matched with antisense nucleotides 745-765 of the gene of xylanase A from *Orpinomyces* PC-2. The underlined and double-underlined nucleotides represent the *Nde*I and *Xho*I restriction sites, respectively. The plasmid pET24(b) with the non-mutated and mutated *xyn*A inserts served as a template.

PCR was performed in a 50 μL volume containing 5 μL 10X buffer, 5 μM of each primer, 2.0 mM of each dNTP, 1.5 unit KOD polymerase, 2.5 mM MgCl2, and 2 ng plasmid DNA. PCR reactions were carried out in a Mastercycler Thermocycler (Eppendorf, Germany) with the following conditions: initial heating at 94 °C for 3 min, then 3 cycles of 95 °C for 20 s, 37 °C for 30 s and 72 °C for 60 s, then 30 cycles of 95 °C for 20 s, 65 °C for 30 s and 72 °C for 45 s, followed by a 72 °C incubation period for 10 min.

2.5. Cloning and sequence analysis

The PCR product was visualized on a 0.8% (w/v) agarose gel, purified using the Gel Extraction kit, digested with *Nde*I and *Xho*I and cloned into the expression vectors pET24b(+) using the T4 DNA ligase kit. The ligated product was used to transform *E. coli* DH5α. The recombinant plasmidial DNA was purified from isolated colonies and verified by DNA sequencing with an automatic Macrogen PCR sequencer (Gasan-dong, Geumchun-gu, Seoul Korea).

In order to determine if mutation patterns were maintained, the DNA sequences were translated into their protein sequences and compared to the initial sequences using the CLUSTALW (Version 1.81) alignment program (http://www.ebi.ac.uk/clustalw). Plasmidial DNAs were then extracted from *E. coli* DH5α and transferred by thermal shock protocol to *E. coli* BL21-CodonPlus(DE3)-RIPL.

2.6. Xylanase expression

E. coli cultures (1 mL) were initially inoculated in 40 mL of LB/Kan medium (triptone 1%, NaCl 1%, yeast extract 0.5%) and shaken overnight at 250 rpm and 37 °C (New Brunswick, Scientific Co., Edison, NJ, USA). A total of 40 mL of the cultures were inoculated in 1L of SOB/Kan media (triptone 2%, yeast extract 0.5%, NaCl 0.05%, KCl 2.5 mM, MgSO4 0.01 M, NaOH 0.5 mM) and shaken at 250 rpm and 37 °C until the OD_{600} reached 1.0. After that, 2.5 mL of IPTG solution (100 mM) were added to 1L cultures (final concentration of 0.25 mM) and shaken at 37 °C, 250 rpm for 4 h to induce xylanase expression.

After induction, the cultures were incubated on ice for 30 min and then centrifuged (15,000 × *g*) at 4 °C for 30 min. The pellet was resuspended in 25 mL of sodium phosphate buffer, 100 mM, pH 6.5. The intracellular xylanase preparations were obtained after sonication cycles of thirty times for 10 s with a break of 10 s between each sonication. This suspension was then centrifuged at 4 °C and

15,000 × *g* for 20 min, and the supernatant was used as an crude enzyme extract.

2.7. Intracellular xylanases purification

The intracellular xylanases were loaded into a Q-Sepharose ion exchange column (1.6 × 2.5 cm) (GE Healthcare Life Sciences, Uppsala, Sweden) previously equilibrated with 25 mM sodium borate buffer, pH 8.5. The sample was also equilibrated and eluted in the same buffer, followed by a linear salt gradient consisting of 25 mM sodium borate buffer, pH 8.5 and the same buffer containing 1 M NaCl. The process was performed by Fast Protein Liquid Chromatography (ÄKTA Protein Purification System – GE Healthcare Life Sciences, Uppsala, Sweden) with a flow rate of 4 mL/min. Active fractions were pooled and analyzed for purity by SDS-PAGE using 12.5% (w/v) acrylamide gel [27]. The protein bands were visualized by silver staining [28].

The protein concentration in the enzymatic extract was determined by the Coomassie Blue binding method using bovine serum albumin (BSA) as the standard [29].

2.8. Mass spectrometry

Mass spectrometric analyses of the WT and SWT xylanases were carried out by matrix-assisted laser desorption-ionization time-of-flight mass spectrometry (MALDI-TOF-MS) method. Purified xylanases were subjected to digestion with sequencing grade modified trypsin (Promega, Madison, MI, USA) according to the An In-Solution Digestion Protocol of Kinter and Shermanet [30]. The peptide fragments were analyzed on AB SCIEX MALDI TOF/TOFTM 5800 System (Applied Biosystems, Foster City, CA, USA). After data acquisition, a list of peaks was obtained from the raw MS/MS data using the 4000 Series Explore Software (Applied Biosystems). The peptide sequences were associated to *m/z* peaks through the theoretical digestion and ionization predicted by MS-digest tool implemented in the ProteinProspector webserver (Version 5.18.1) [31].

2.9. Xylanase assay

Xylanase activity was determined by measuring the release of reducing sugars from beechwood xylan using the dinitrosalicylic acid reagent (DNS) [32]. The xylanase standard assay was performed in 500 μL reaction volumes containing 400 μL (1% w/v) beechwood xylan diluted in 100 mM sodium phosphate buffer pH 6.5 and 0–100 μL of appropriately diluted enzyme preparations. The reaction was carried out for 30 min at 40 °C and stopped by the addition of 0.5 mL of the DNS reagent. Test tubes were boiled for 5 min and then chilled on ice water for 10 min. The amount of reducing sugars released was determined at 540 nm. D-xylose was used as the standard. One unit of xylanase activity was defined as the amount of enzyme that released 1 μmol of xylose per min under standard assay conditions.

The data of xylanase activity were presented as mean values of triplicate assays in which the standard deviations were always less than 10% and the results were expressed as means ± standard deviations.

2.10. Effect of pH, temperature and thermostability on xylanase activity

The influence of pH on xylanase activity was determined under standard assay conditions, except that pH range was from 2.0 to 11.0. The buffers at final concentration of 100 mM were: sodium phosphate buffer (pH values of 2, 3, 7 and 8), sodium citrate buffer (pH 4–6) and sodium carbonate buffer (pH 9–11).

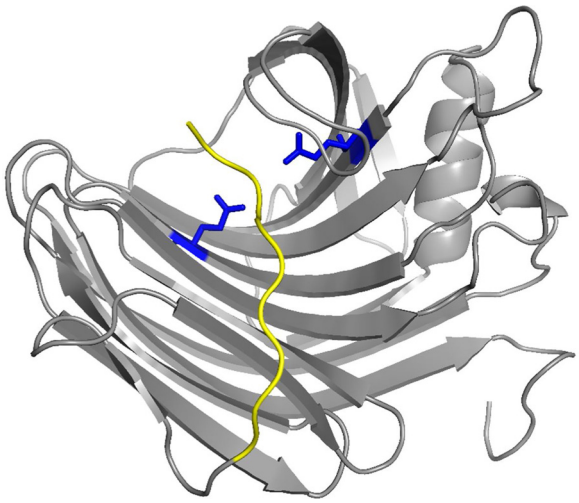

Fig. 1. Homology model of mature xylanase (WT) catalytic domain. The tail that could affect xylanase stability in the N-terminal region is shown in yellow and the two catalytic glutamates are shown in blue sticks. (For interpretation of the references to color in this figure legend, the reader is referred to the web version of this article.)

The effect of temperature on enzyme activity was determined under standard assay conditions, except that temperature ranged from 20 to 80 °C.

Thermal stability was determined by incubating the purified diluted enzyme at 50 °C in 100 mM sodium phosphate buffer, pH 6.5. After incubation at different times, aliquots were removed and the residual xylanase activities were measured by the standard assay. Half-life value of the enzymes was calculated using the CurveExpert program (Version 1.4) [33] from the data of residual activity determined at 50 °C.

2.11. Kinetic properties

The kinetic parameters (k_M and k_{cat}) of the purified xylanases were determined by nonlinear curve fitting using the Michaelis-Menten plot and the CurveExpert program (Version 1.4) [33]. The substrate beechwood xylan was used at concentrations between 0.25 and 10 mg/mL in 100 mM sodium phosphate buffer, pH 6.5 and the assays were carried out at 40 °C for 30 min.

3. Results and discussion

3.1. Molecular dynamics simulations and small xylanase evaluation

Prediction analyzes of the export signal peptide and the cleavage site from *Orpinomyces* XynA xylanase identified a processing site between amino acid residues 18 and 19 to generate the mature enzyme.

The molecular dynamics analysis of the mature WT xylanase revealed that the first ten residues in the N-terminal region have no defined secondary structure, weakly to interact with the remaining global structure and high mobility, reaching amino acids near the catalytic site. Therefore, we suggest that removal of this N-terminal tail could improve the stability of the molecule. Fig. 1 shows the mature WT xylanase 3D structure, emphasizing the N-terminal destabilizing region.

In order to verify if removal of this region would compromise the xylanase activity, a MD trajectory of 10 ns was evaluated to investigate the average RMS fluctuations of amino acids (Fig. 2). It is seen that the majority of the residues of the small xylanase (SWT – mature xylanase without the first ten amino acids) showing dis-

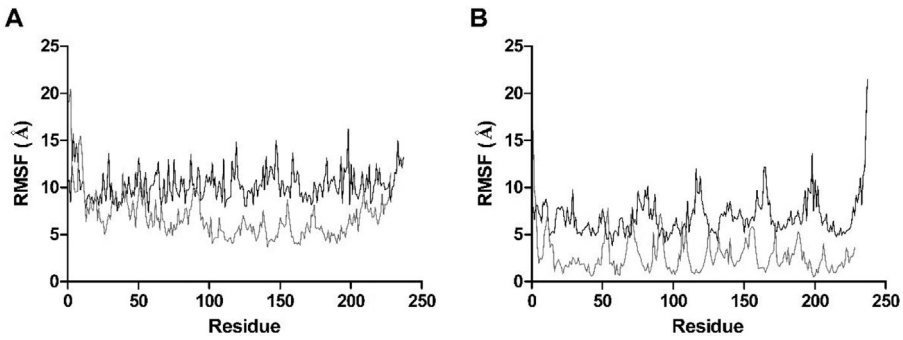

Fig. 2. Average RMS fluctuation values (Å) as a function of amino acid sequence up to 10 ns simulation trajectory at 313 K (A) and 323 K (B). Mature xylanase WT (black); small xylanase SWT, without the N-terminal tail (gray).

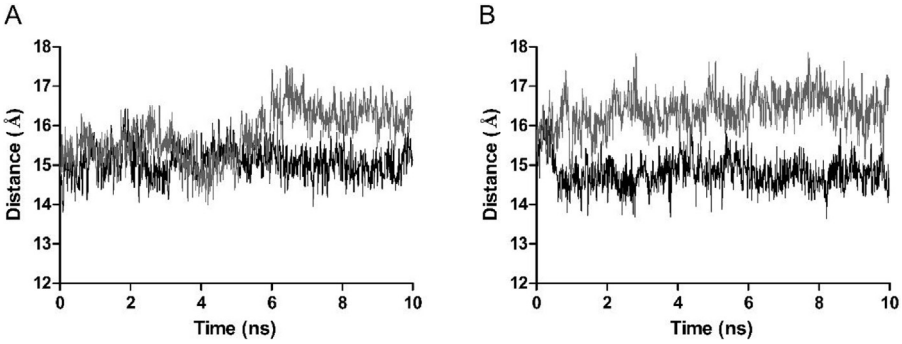

Fig. 3. Distance (Å) between the catalytic glutamate residues of the xylanases along a molecular dynamic trajectory of 10 ns at 313 K (A) and 323 K (B). Mature xylanase WT (black); small xylanase SWT, without the N-terminal tail (gray).

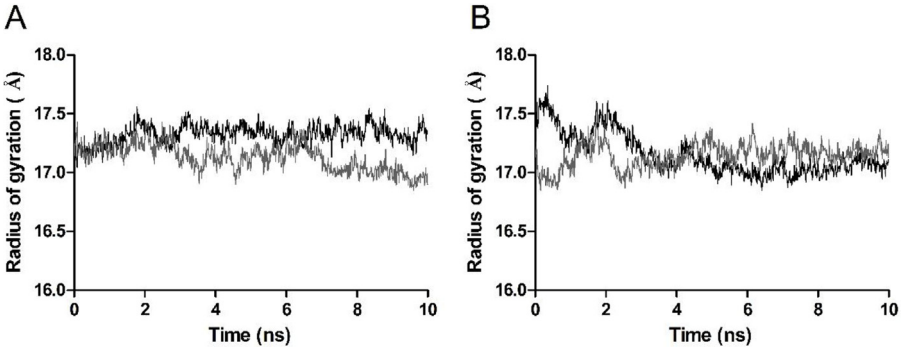

Fig. 4. Radius of gyration (Å) of the xylanases along a molecular dynamic trajectory of 10 ns at 313 K (A) and 323 K (B). Mature xylanase WT (black); small xylanase SWT, without the N-terminal tail (gray).

placements less than 9.0 Å at 313 K and less than 5.0 Å at 323 K. On the other hand, the RMS fluctuations observed for amino acids located in the most stable conformations of β-sheets and α-helix of mature xilanase (WT) were higher than the observed displacements for all residues of SWT. This result indicated that removal of the N-terminal tail could promote the stabilization of individual residues and of the whole molecule.

The distance between the catalytic glutamate residues (E115 and E203) of the SWT and WT (E124 and E212) was evaluated (Fig. 3). Positioning of the catalytic residues on the active site, during simulations at both evaluated temperatures, suggests that the tail removal promoted considerable structural changes in the active site, resulting in a gain of flexibility in the SWT, which probably ensures the catalytic performance of this enzyme.

The radius of gyration (Rg) of the mature xylanase WT and small xylanase SWT were presented in Fig. 4. The Rg is a parameter that describes the equilibrium conformation of a total system, indicating protein structure compactness [34]. The lower Rg value, presented by the SWT structure at 313 K, indicates that the small enzyme has a more compact structure which may have implications on the overall protein stability, while at 323 K both xylanases acquired similar Rg values.

The information obtained from molecular dynamics analyses indicated that removal of the N-terminal tail could promote increased enzyme stability, since this N-terminal region have no defined secondary structure that appears highly flexible. Besides that, the N-terminal tail location near catalytic amino acids in the 3D structure of the xylanase molecule (Fig. 1), suggest that this tail can also influence the proper positioning of the substrate in the cavity of the catalytic site, which could result in reduced enzymatic activity.

3.2. N-terminal evaluation by mass spectrometry

In order to confirm the differences in the N-terminal region of the xylanases, the genes encoding the WT and SWT were cloned into the expression vector pET24(b) and used to transform *E. coli* BL21(DE3)RIPL. The expressed enzymes were purified, digested and

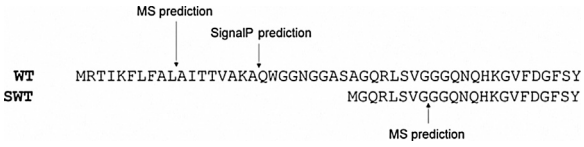

Fig. 5. N-terminal region of the WT and SWT xylanases with the respective signal peptide processing sites predicted by SignalP Server and by MS.

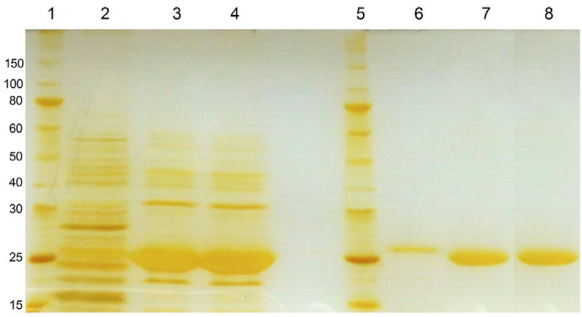

Fig. 6. SDS-PAGE (12.5%) of the *E. coli* intracellular crude extract and purified xylanases. 1–molecular weight marker, 2–protein profile from expression of WT 3–protein profile from expression of SWT, 4–protein profile from expression of SM2, 5–molecular weight marker, 6–purified WT, 7–purified SWT, 8–purified SM2. Protein gel was stained with silver nitrate.

analyzed by mass spectrometry (MALDI-TOF-MS). The analyses of the identified peptides suggest that processing of signal peptide by *E. coli* occurred at a cleavage site different from that predicted by SignalP (Fig. 5). Based on the predictions of SignalP, the size difference between WT and SWT xylanases would be equivalent to nine amino acid residues, which could form a small loop at the N-terminal region of WT. On the other hand, the analyses of the identified peptides showed that these enzymes expressed in *E. coli* exhibited a difference of 25 amino acid residues. This sequence of 25 amino acid residues could form an unstructured loop, which could negatively affect the positioning of the substrate in the catalytic cavity, reducing the enzymatic activity of WT.The MS analyses showed the peptides of 697.909 *m*/*z* and 807.139 *m*/*z*, which were obtained from WT and SWT fragmentation, respectively (Fig. S1). These peptides were incompatible with the expected products from tryptic cleavage of these xylanases. The 697.909 *m*/*z* was compatible with the AITTVAK fragment, which is part of the expected FLFALAITTVAK peptide. Similarly, the 807.139 *m*/*z* was equivalent to the GGQNQHK fragment, which is part of the LSVGGGQNQHK peptide. These results indicate that the processed signal peptide of WT corresponded to the first ten amino acid residues, while the processed signal peptide of SWT was corresponding to the first eight amino acid residues (Fig. 5). Therefore, it is possible to assume that the difference in mass between these enzymes would be equivalent to 25 amino acid residues. This variation in molecular mass of WT and SWT xylanases was confirmed by SDS-PAGE (Fig. 6). The protein band corresponding to purified WT xylanase (lane 6) presented higher molecular mass compared to purified SWT band (lane 7). These observations are in agreement with the WT and SWT molecular masses estimated by ProtParam, that were 26,640.48 Da and 24,300.89 Da, respectively.

3.3. The effect of tail removal on xylanase properties

The specific activity determined from crude enzyme extracts of WT and SWT xylanases were significantly different. The specific activity of SWT was 3,752.1 U mg^{-1} of protein, while at the same conditions the specific activity of WT was 231.7 U mg^{-1} of protein.

The protein profile of the intracellular crude extracts from *E. coli* expressing WT or SWT (Fig. 6) showed that SWT was the most abundant protein in the crude extract (lane 3), while the amount of WT was relatively low and similar to several other proteins expressed from *E. coli* (lane 2). In this way, the higher concentration of SWT in the active protein extract could contribute to its superior specific activity, however other factors are involved, which could explain the difference in the specific activity of these xylanases.

Various studies have shown that the N-terminal region of GH11 xylanases is related to enzyme stability [11] and recent molecular dynamic information has indicated that protein unfolding initiates there [35]. *E. coli* has the N-end rule pathway, which relates the *in vivo* half-life of a protein to the identity of its amino-terminal residue. It was shown that unstable proteins contained Arg, Lys, Phe, Leu, Trp and Tyr at the amino terminus [36,37]. In our findings, the presence of destabilizing amino acid residues in the xylanase N-terminal could reduce the protein stability. In fact, the N-terminal region of WT is highly rich in Arg, Lys, Phe and Leu residues (AAD04194). Degradation of WT xylanase could occur prior to signal peptide processing in the periplasm, as observed in expression systems of recombinant proteins by *E. coli* [37,38]. This amino terminus region could potentially contribute to lower stability and reduced specific activity of the WT, however other factors that affect the expression of the enzymes may be involved [11,37].

These enzymes were purified using ion exchange chromatography and the electrophoretic profile of these purified xylanases confirmed the presence of a single protein band of WT and SWT (Fig. 6). The specific activities of purified SWT and WT were 5,801.7 U mg^{-1} of protein and 444.1 U mg^{-1} of protein, respectively. This higher specific activity of SWT indicates that the removal of residues in the N-terminal region could promote an improvement in xylanase activity. In sum, it seems that the N-terminal tail removal positively affected the expression and activity of SWT.

Based on this information, we decided to use the N-terminal region removal approach to evaluate its effect on a mutant xylanase, also derived from *Orpinomyces* XynA.

3.4. Production of a mutant small xylanase

The mutant xylanase M2 (V135A, A226T) was previously obtained by directed evolution [9]. The M2 enzyme presented improved thermostability at 50 and 60 °C, but its activity in the *E. coli* intracellular crude extract was 34.4 U mg^{-1} of protein [9]. In order to increase the expression and activity of a more stable xylanase, the N-terminal region of the M2 xylanase was removed, generating the small xylanase SM2. After introduction of a methionine residue (start codon) to ensure successful protein synthesis, gene sequencing indicated that the mutation pattern introduced previously was maintained. The new small enzyme was expressed in *E. coli* BL21(DE3)RIPL and the SM2 activity in the intracellular crude extract reached 2,846.8 U mg^{-1} of protein. After purification, the SM2 enzyme showed specific activity of 5,106.8 U mg^{-1} at 40 °C, pH 6.5.

3.5. Characterization of xylanases

The purified WT, SWT and SM2 xylanases had an optimum temperature at 60 °C and showed similar behavior at temperatures from 20 to 80 °C (Fig. 7A). This value of optimal temperature was the same as that exhibited by M2 xylanase [9], and by *Bacillus subtilis* xylanase [39], and higher than several fungi xylanases that present optimal activities at temperatures below 45 °C [40,41].

The WT, SWT and SM2 showed optimum pH within the range of 5–8 (Fig. 7B). It is interesting to highlight that the SWT showed considerable residual activity when assayed in pH 9, about 50%, while the residual activity of WT and SM2 were around 10% and 30%, respectively. SM2, WT and SWT enzymes showed considerable

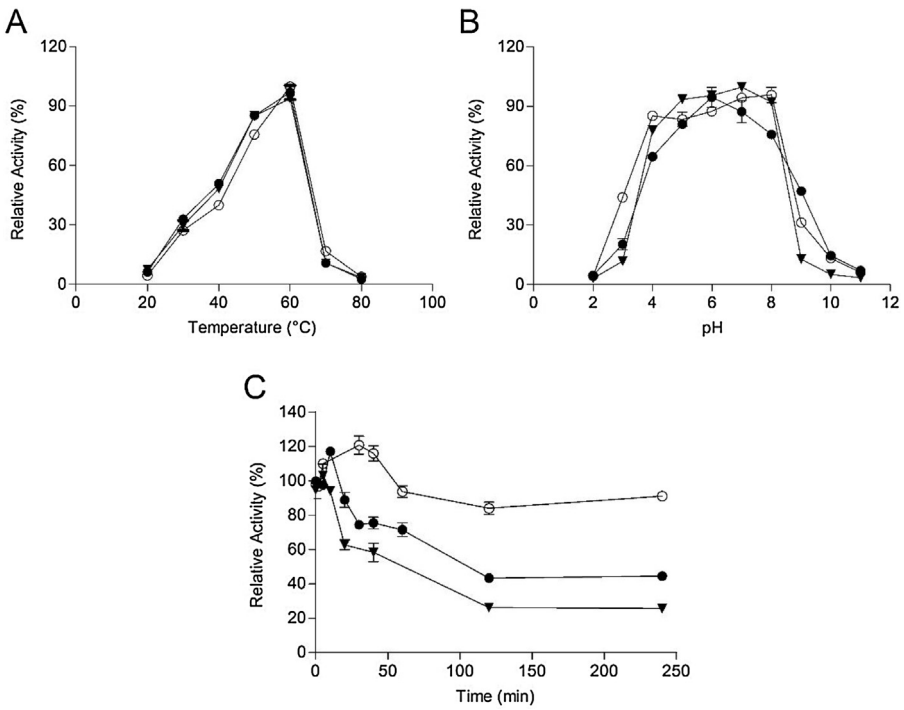

Fig. 7. A – Effect of temperature on WT, SWT and SM2 activity at pH 6.5. The xylanase activity was measured under temperatures ranging from 20 to 80 °C. B – Effect of pH on WT, SWT and SM2 activity at 40 °C. Xylanase activity was measured under pH values ranging from 2.0 to 11.0. C – Thermostability at 50 °C. Relative activity is expressed as a percentage of the maximum enzyme activity under standard assay conditions. All data plotted are average of triplicates. WT (▼), SWT (●), SM2 (○).

Table 1
Properties of xylanases. The values of half-life ($t_{1/2}$), k_M and k_{cat} constants were determined from activity standard assay, using purified xylanases and beechwood xylan as substrate.

Enzymes	$t_{1/2}$ at 50 °C (h)	k_M (mg mL^{-1})	k_{cat} (min^{-1})	k_{cat}/k_M (mL/min^{-1} mg^{-1})
WT	0.77	1.05	8.0×10^6	8.0×10^6
SWT	2.27	0.73	2.3×10^9	3.3×10^9
SM2	29.46	0.62	1.8×10^{10}	2.9×10^{10}

residual activity when assayed in a wide pH range from acidic to alkaline pH values, similar to xylanases from other sources [40,41]. The SM2 retained approximately 45% of its maximal xylanase activity at pH 3 (Fig. 7B). These xylanases could be more suitable for biotechnological applications that require acidic and neutral pH conditions. For industrial applications, it is interesting that the xylanases exhibit greater activity in a wide pH range and high temperature. However, natural xylanases that are thermostable and acid or alkali tolerant are limited [42].

As expected, the SM2 was the enzyme more thermostable at 50 °C, followed by SWT and WT xylanase (Fig. 7C). Half-life values of the SM2, SWT and WT at 50 °C were 1,767.6 min, 136.4 min and 46.0 min, respectively. After 20 min of incubation at 50 °C the WT maintained 62.8% of its activity, and after 2 h of incubation this enzyme exhibited about 26.2% of its original activity. On the other hand, the SWT retained 88.8% of its activity after 20 min of incubation at the same conditions, and after 2 h the residual activity was still approximately 43.3%. Already the xylanase SM2 maintained 90% activity even after 4 h incubation. The N-terminal tail removal could promote structural changes in these molecules that could increase the thermal stability at 50 °C.

Chen et al. [8] purified and characterized the native xylanase from *Orpinomyces* sp. PC-2. The crude culture fluid presented a specific activity of 11.2 U mg^{-1} of protein and the specific activity of the purified enzyme was 1,560.0 U mg^{-1} of protein. The enzyme was most active at temperatures of 40–50 °C and pH from 5.0 to 6.6. So, the expression of the xylanases derived from *Orpinomyces* XynA in *E. coli* combined with the N-terminal tail removal promoted an increase in the production of xylanases with gain of activity and stability.

The k_M values of purified xilanases were calculated by the Michaelis-Menten plot using beechwood xylan as the substrate (Table 1). The k_M values for the SWT and SM2 were close to each other (0.73 and 0.62 mg mL^{-1}, respectively) and both were lower than the k_M value of WT xylanase (1.05 mg mL^{-1}), indicating that small xylanases presented higher affinity for the substrate. Values of k_{cat}/k_M, a parameter that evaluates the catalytic efficiency of the enzymes, were 8.0×10^6 for WT, 3.3×10^9 for SWT and 2.9×10^{10} for SM2. These results highlight that tail removal greatly enhanced the catalytic efficiency of the enzymes to catalyze the hydrolysis of beechwood xylan.

Several studies have focused on changes in the N-terminal region to improve the thermostability of xylanases [11,43,44]. Yin et al. [43] replaced the N-terminal segment of a mesophilic GH11 xylanase from *Aspergillus oryzae* (AoXyn11) by the corresponding region of a hyperthermotolerant GH11 xylanase (EvXyn11TS) and the modified xylanase was highly improved and showed optimum temperature at 75 °C and high thermostability at 65 °C. Song et al. [44] obtained a more active xylanase by the addition of 17 amino acids to the N-terminal of GH11 xylanase from *Thermobacillus xylanilyticus*. On the other hand, the removal of un-structured residues in the N-terminal region resulted in the reduction of the optimum temperature and thermostability of an *Aspergillus niger* GH11 xylanase [11]. Thus, removal of this N-terminal tail proved

to be advantageous, since it promoted an increase in enzyme stability, catalytic efficiency as well as marked an increase in xylanase production, achieving considerable levels of expression. These improved xylanases would have potential for biotechnological applications, especially in processes that require more active and stable enzymes.

4. Conclusions

Molecular dynamics simulations contributed to the identification and evaluation of a destabilizing N-terminal tail on *Orpinomyces* WT xylanase. Two xylanases codified by xynA gene without these N-terminal destabilizing residues, one mutated (SM2) and the other non-mutated (SWT), were expressed at high levels in *E. coli*. These enzymes were more active and stable when compared to WT xylanase in a broader range of pH and temperature. The positive effect of tail removal on xylanases catalytic properties reproduced the predictions performed by the MD analyzes. The properties of these improved xylanases suggest the potential of applying in several biotechnological applications.

Conflict of interest

The authors report no conflicts of interest.

Acknowledgments

This work was supported by grants from the Fundação de Amparo à Pesquisa do Estado de Minas Gerais-FAPEMIG, the Coordenação de Aperfeiçoamento de Pessoal de Nível Superior-CAPES and Conselho Nacional de Desenvolvimento Científico e Tecnológico-CNPq, Brazil. The authors thank Dr. Douglas B. Jordan from the USDA, ARS, NCAUR, Peoria, IL, and Dr. Xin-Liang Li for their technical support.

Appendix A. Supplementary data

Supplementary data associated with this article can be found, in the online version, at http://dx.doi.org/10.1016/j.ijbiomac.2017.08.015.

References

[1] X. Jia, W. Qiao, W. Tian, X. Peng, S. Mi, H. Su, Y. Han, Biochemical characterization of extra- and intracellular endoxylanse from thermophilic bacterium *Caldicellulosiruptor kronotskyensis*, Sci. Rep. 6 (2016) 1–12.
[2] G. Paës, J.G. Berrin, J. Beaugrand, GH11 xylanases: structure/function/properties relationships and applications, Biotechnol. Adv. 30 (2012) 564–592.
[3] B. Henrissat, M. Vegetales, F. Grenoble, A classification of glycosyl hydrolases based sequence similarities amino acid, Biochem. J. 280 (1991) 309–316.
[4] V. Lombard, H. Golaconda Ramulu, E. Drula, P.M. Coutinho, B. Henrissat, The carbohydrate-active enzymes database (CAZy) in 2013, Nucleic Acids Res. 42 (2014) 490–495.
[5] J. Álvarez-Cervantes, G. Díaz-Godínez, Y. Mercado-Flores, V.K. Gupta, M.A. Anducho-Reyes, Phylogenetic analysis of β-xylanase SRXL1 of *Sporisorium reilianum* and its relationship with families (GH10 and GH11) of Ascomycetes and Basidiomycetes, Sci. Rep. 6 (2016) 1–9.
[6] D.S. Vieira, L. Degrève, R.J. Ward, Characterization of temperature dependent and substrate-binding cleft movements in *Bacillus circulans* family 11 xylanase: a molecular dynamics investigation, Biochim. Biophys. Acta 1790 (2009) 1301–1306.
[7] X.-L. Li, L.G. Ljungdahl, H. Chen, Orpinomyces xylanase proteins and coding sequences, 5,824,533 (Patent), 1998.
[8] H.Z. Chen, X.-L. Li, L.G. Ljungdahl, Purification and characterization of an endoxylanase form the anaerobic polycentric rumen fungus *Orpinomyces* sp. strain PC-2, SAAS Bull. Biochem. Biotechnol. 12 (1999) 7–14.
[9] L.M. Trevizano, R.Z. Ventorim, S.T. de Rezende, F.P.S. Junior, V.M. Guimarães, Thermostability improvement of *Orpinomyces* sp. xylanase by directed evolution, J. Mol. Catal. B: Enzym. 81 (2012) 12–18.
[10] H. Xue, J. Zhou, C. You, Q. Huang, H. Lu, Amino acid substitutions in the N-terminus, cord and α-helix domains improved the thermostability of a family 11 xylanase XynR8, J. Ind. Microbiol. Biotechnol. 39 (2012) 1279–1288.
[11] L. Liu, X. Sun, P. Yan, L. Wang, H. Chen, Non-structured amino-acid impact on GH11 differs from GH10 xylanase, PLoS One 7 (2012) 1–6.
[12] T.N. Petersen, S. Brunak, G. von Heijne, H. Nielsen, Signal P4.0: discriminating signal peptides from transmembrane regions, Nat. Methods (2011) 785–786.
[13] E. Gasteiger, C. Hoogland, A. Gattiker, S. Duvaud, M.R. Wilkins, R.D. Appel, A. Bairoch, Protein identification and analysis tools on the ExPASy server, Proteom. Protoc. Handb. (2005) 571–607.
[14] L.A. Kelley, S. Mezulis, C.M. Yates, M.N. Wass, M.J.E. Sternberg, The Phyre2 web portal for protein modelling, prediction and analysis, Nat. Protoc. 10 (2015) 845–858.
[15] M. Vardakou, C. Dumon, J.W. Murray, P. Christakopoulos, D.P. Weiner, N. Juge, R.J. Lewis, H.J. Gilbert, J.E. Flint, Understanding the structural basis for substrate and inhibitor recognition in eukaryotic GH11 xylanases, J. Mol. Biol. 375 (2008) 1293–1305.
[16] R.A. Laskowski, M.W. MacArthur, D.S. Moss, J.M. Thornton, PROCHECK: a program to check the stereochemical quality of protein structures, J. Appl. Crystallogr. 26 (1993) 283–291.
[17] J.U. Bowie, R. Luthy, D. Eisenberg, A method to identify protein sequences that fold into a known three-dimensional structure, Science 253 (1991) 164–170.
[18] R. Luthy, J.U. Bowie, D. Eisenberg, Assessment of protein models with three-dimensional profiles, Nature 356 (1992) 83–85.
[19] C. Colovos, T.O. Yeates, Verification of protein structures: patterns of nonbonded atomic interactions, Protein Sci. 2 (1993) 1511–1519.
[20] S.C. Lovell, I.W. Davis, W.B. Adrendall, P.I.W. de Bakker, J.M. Word, M.G. Prisant, J.S. Richardson, D.C. Richardson, Structure validation by C alpha geometry: phi, psi and C beta deviation, Proteins-Struct. Funct. Genet. 50 (2003) 437–450.
[21] M. Wiederstein, M.J. Sippl, ProSA-web: interactive web service for the recognition of errors in three-dimensional structures of proteins, Nucleic Acids Res. 35 (2007) 407–410.
[22] A. Drozdetskiy, C. Cole, J. Procter, G.J. Barton, JPred4: a protein secondary structure prediction server, Nucleic Acids Res. 43 (2015) W389–W394.
[23] J.C. Phillips, R. Braun, W. Wang, J. Gumbart, E. Tajkhorshid, E. Villa, C. Chipot, R.D. Skeel, L. Kalé, K. Schulten, Scalable molecular dynamics with NAMD, J. Comput. Chem. 26 (2005) 1781–1802.
[24] A. MacKerell, D. Bashford, M. Bellot, R. Dunbrack, J. Evanseck, M. Field, S. Fischer, J. Gao, H. Guo, S. Ha, D. Joseph-McCarthy, L. Kuchnir, K. Kuczera, F. Lau, C. Mattos, S. Michnick, T. Ngo, D. Nguyen, B. Prodhom, W. Reiher, B. Roux, M. Schlenkrich, J. Smith, R. Stote, J. Straub, M. Watanabe, J. Wiorkiewicz-Kuczera, D. Yin, M. Karplus, All-atom empirical potential for molecular modeling and dynamics studies of proteins, J. Phys. Chem. B 102 (1998) 3586–3616.
[25] W. Humphrey, A. Dalke, K. Schulten, VDM: visual molecular dynamics, J. Mol. Graph. 14 (1996) 33–38.
[26] T. Darden, D. York, L. Pedersen, Particle mesh Ewald: an N log(N) method for Ewald sums in large systems, J. Chem. Phys. 98 (1993) 10089.
[27] U.K. Laemmli, Cleavage of structural proteins during the assembly of the head of bacteriophage T4, Nature 227 (1970) 680–685.
[28] H. Blum, H. Beier, H.J. Gross, Improved silver staining of plant proteins, RNA and DNA in polyacrylamide gels, Electrophoresis 8 (1987) 93–99.
[29] M.M. Bradford, A rapid and sensitive method for the quantitation of microgram quantities of protein utilizing the principle of protein-dye binding, Anal. Biochem. 72 (1976) 248–254.
[30] M. Kinter, N.E. Sherman, The preparation of protein digests for mass spectrometric sequencing experiments, in: D.M. Desiderio, N.M.M. Nibbering (Eds.), Protein Seq. Identif. Using Tandem Mass Spectrom, first edition, Wiley-Interscience, Inc., New York, 2000, pp. 147–165.
[31] R.J. Chalkley, P.R. Baker, K.F. Medzihradszky, A.J. Lynn, A.L. Burlingame, In-depth analysis of tandem mass spectrometry data from disparate instrument types, Mol. Cell. Proteom. 7 (2008) 2386–2398.
[32] G.L. Miller, Use of dinitrosalicylic acid reagent for determination of reducing sugar, Anal. Chem. 3 (1959) 426–428.
[33] D.G. Hyams, CurveExpert. http://www.curveexpert.net (2010).
[34] M.Y. Lobanov, N.S. Bogatyreva, O.V. Galzitskaya, Radius of gyration as an indicator of protein structure compactness, Mol. Biol. 42 (2008) 623–628.
[35] M. Purmonen, J. Valjakka, K. Takkinen, T. Laitinen, J. Rouvinen, Molecular dynamics studies on the thermostability of family 11 xylanases, Protein Eng. Des. Sel. 20 (2007) 551–559.
[36] J.W. Tobias, T.E. Shrader, G. Rocap, The N-end rule in bacteria Ub-X-Pgal, Science 254 (1991) 1374–1377.
[37] M. Fakruddin, R.M. Mazumdar, K.S. Bin Mannan, A. Chowdhury, M.N. Hossain, Critical factors affecting the success of cloning, expression, and mass production of enzymes by recombinant *E. coli*, ISRN Biotechnol. 2013 (2013) 1–7.
[38] L.C. Simmons, D.G. Yansura, Translational level is a critical factor for the secretion of heterologous proteins in *Escherichia coli*, Nat. Biotechnol. 14 (1996) 629–634.
[39] M. Saleem, F. Aslam, M.S. Akhtar, M. Tariq, M.I. Rajoka, Characterization of a thermostable and alkaline xylanase from *Bacillus* sp. and its bleaching impact on wheat straw pulp, World J. Microbiol. Biotechnol. 28 (2012) 513–522.
[40] A. Krisana, S. Rutchadaporn, G. Jarupan, E. Lily, T. Sutipa, K. Kanyawim, Endo-1,4-β-xylanase B from *Aspergillus* cf. *niger* BCC14405 isolated in Thailand: purification, characterization and gene isolation, J. Biochem. Mol. Biol. 38 (2005) 17–23.

[41] S. Leskinen, A. Mäntylä, R. Fagerström, J. Vehmaanperä, R. Lantto, M. Paloheimo, P. Suominen, Thermostable xylanases, Xyn10A and Xyn11A, from the actinomycete *Nonomuraea flexuosa*: isolation of the genes and characterization of recombinant Xyn11A polypeptides produced in *Trichoderma reesei*, Appl. Microbiol. Biotechnol. 67 (2005) 495–505.
[42] B.K. Bajaj, M. Sharma, S. Sharma, Alkalistable endo-β-1,4-xylanase production from a newly isolated alkalitolerant *Penicillium* sp. SS1 using agro-residues, 3 Biotec 1 (2011) 83–90.
[43] X. Yin, J.-F. Li, J.-Q. Wang, C.-D. Tangaand, M.-C. Wu, Enhanced thermostability of a mesophilic xylanase by N-terminal replacement designed by molecular dynamics simulation, J. Sci. Food Agric. 93 (2013) 3016–3023.
[44] L. Song, C. Dumon, B. Siguier, I. André, E. Eneyskaya, A. Kulminskaya, S. Bozonnet, M.J. O'Donohue, Impact of an N-terminal extension on the stability and activity of the GH11 xylanase from *Thermobacillus xylanilyticus*, J. Biotechnol. 174 (2014) 64–72.